

Investigation of a Submerged Cavitating Jet Behaviour: Part Two – Influences of Operating Conditions, Geometrical Parameters and Arrangements of Detection System

Ezddin Ali Farag Hutli
Ph.D. Student

Miloš S. Nedeljković
Professor
University of Belgrade
Faculty of Mechanical Engineering

In visualization results of highly-submerged cavitating water jet obtained by a digital camera, the influences of parameters such as: injection pressure, nozzle diameter and geometry, nozzle mounting (convergent or divergent), cavitation number and exit jet velocity, were investigated. In addition, the position of visualization system was studied. All the parameters have been found to be of strong influence on the jet appearance and performance.

Keywords: Cavitating jet, cavitation cloud, cavitation ring, vapor cavity, gas cavity, cavitation number, divergent, convergent.

1. INTRODUCTION

Over the past few years, cavitating fluid jets have received a considerable attention, primarily with laboratory experiments, to understand their behaviour and to determine the feasibility of their use in a variety of situations. Recently, these testing and evaluation efforts have proven certain applications of the cavitating jet, which include: cleaning paint and rust from metal surfaces; underwater removal of marine fouling; removing of high explosives from munitions; augmenting the action of deep-hole mechanical bits used to drill for petroleum or geothermal energy resources; widely use in cutting, penning and flushing. Thus cavitating fluid jet method is indeed commercially attractive - Soyama H. et al. (1994), Vijay M. et al. (1991), and Conn A. et al. (1981).

If the unsteady behavior and the jet structure are clarified in detail, expectedly, the jet working capacity may be drastically improved - Soyama H. et al. (1994), Vijay M. et al. (1991). The cavitation clouds in general behave stochastically both in time and space, with a very rapid change within μs - Ganippa L.C. et al. (2001), Soyama H. et al. (1994), Ito Y. et al. (1988), Caron J. et al. (1995), Clanet C. (1995), Koivula T. (2000), Vijay M. et al. (1991), and Oba R. (1994).

Other researchers like Soyama H. et al. (1995, 2005), Keiichi and Yasuhiro (2002) found from their studies that phenomenon is periodical and it depends on many parameters such as hydrodynamic conditions and geometry of facility.

Kato H. et al. (1999) used laser holograph to observe and visualize the cavitation cloud on a foil. They

visualized the U-shaped vortex cavitation surrounded by many bubbles and concluded that this is the main feature of their case of cavitation.

Toyoda K. et al. (1999) investigated the vortical structure of a circular water jet using a laser fluorescent dye and a laser light sheet. Their results of visualization show that the streamwise vortices have fundamental effect on the entrainment of ambient fluid.

In this paper a normal digital camera was used for visualization and investigation of the influences of hydrodynamic conditions, nozzle geometry, and position of the visualization system.

2. EXPERIMENTAL SETUP AND MEASUREMENT PROCEDURE

The experimental set-up for jet performance investigation and its look have been shown in Part 1 of this paper.

Hydrodynamic conditions are settled on to produce cavitating jet. The intensity of cavitating jet is controlled via the upstream pressure and downstream pressure, which are measured precisely by transducers and controlled using the needle valves (regulation valves). The nozzle may be mounted in a holder in two ways regarding the inlet and outlet diameters: divergent and/or convergent conicity – Fig.1 shows holder and the nozzle mounting.

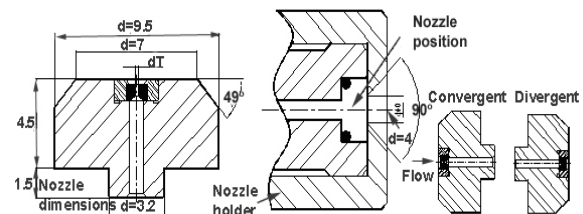


Figure 1. Nozzle geometry (dimensions mm), nozzle holder, directions of nozzle mounting.

Received: November 2007, Accepted: December 2007

Correspondence to: Dr Miloš Nedeljković

Faculty of Mechanical Engineering,
Kraljice Marije 16, 11120 Belgrade 35, Serbia
E-mail: mnedeljkovic@mas.bg.ac.yu

3. VISUALIZATION OF CAVITATING JETS USING NIKON DIGITAL CAMERA

The visualization investigations of the cavitating jets were done using NIKON COOLPIX 990 digital camera and Strobex CHADWICK stroboscope of duration time $30 \mu\text{s}$ to illuminate the cavitating jet. The angle (θ) between the flash and the camera eye was $\theta = 90^\circ$ and the angle between the jet flow direction and the flash was $\phi = 90^\circ$ (the center of the center line of the jet path along the jet length is used as a reference point of measuring the different angles). Scheme of the visualization system is shown in Fig.2. Three nozzles of different diameters were used to investigate the influences of downstream pressure, upstream pressure and nozzle geometry on the characteristics of cavitating jets. The flash frequency was 50 Hz and was chosen in order to be compatible with or near to the shutter camera frequency $1/30$ or $1/60 \text{ s}^{-1}$. The jet images were taken as a movie where the movie contains around 600 frames in 40 s (15 frames/s). Then the jet behavior has been followed by extracting appropriate images.

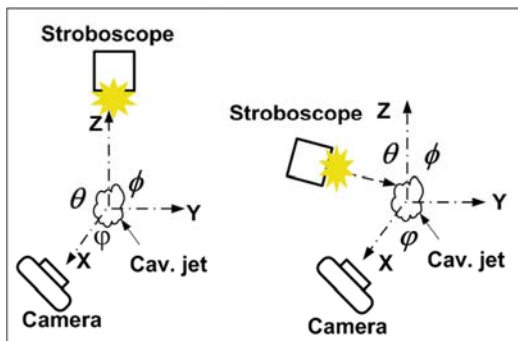


Figure 2. Arrangement of the apparatus used in visualization process. The angles between the stroboscope and the camera are shown.

3.1 Influence of Nozzle Conicity

The visualization of the cavitating jet was done for two cases of mounting of the nozzle in the holder - divergent and convergent mounting - Fig. 1.

From the analysis of the group of the images for both cases, it may be concluded that the hydrodynamic conditions have a big influence on the jet behaviour and its features, where as the upstream pressure increases the jet penetration also increases, and the breaking point is shifted to downstream. In addition, the length of cavitating jet clouds increases too.

Fig.3 shows the first group of images of cavitating jet at low upstream pressure (p_1). Visualization results reveal that the jet is comprised only of very tiny individual bubbles with wide spreading angle. The existence of tiny bubbles is attributed to the inception of cavitation inside the nozzle instead at the nozzle outlet (as in the case of convergent nozzle).

The groups of images in Figs. 4 and 5, which are for divergent and convergent respectively, show that cavitation started to go out from the nozzle as a dense

cloud and diffused immediately into light clouds, which look smoky in appearance.

At upstream pressure of $p_1 = 45 \text{ bar}$, the jet clouds exist (penetrate) only to the maximum distance of 20% of the distance between the nozzle lip and the target surface (which is denoted by x , $x = 25.67 \text{ mm}$). As the upstream pressure increases, for both cases the jet penetration is increased and arrives to the target wall in the form of strong clouds (these clouds create erosion on the exposed target surface). At the same time the jet starts to be denser (dense clouds with cluster bubbles result from the jet breaking off and many individual liberated bubbles, i.e. individual cavities with a short life time). The positions of jet breaking-off points are shifted downstream, and the spreading angles of the jet are decreased. When the jet is destroyed before the target, it spreads radially and covers the target area with white smoky clouds containing very tiny bubbles. However, when the jet strikes the target wall (big cavity clouds) it will be destroyed and the water which covers the target is reflected back as a ring. The ring also contains the bubbles which were directed that way in the process of jet cloud destruction. These rings are not responsible for the production of ring erosion. The ring pattern erosion comes as a result of the clouds destruction (to many small bubbles) due to collision with the target wall. These bubbles are distributed radially along the target area and when the bubbles meet higher-enough pressure they collapse. Since the bubbles do not have the same size and composition, they do not have the same strength, and this is the reason why there are different degrees of hole depth along the erosion ring diameter.

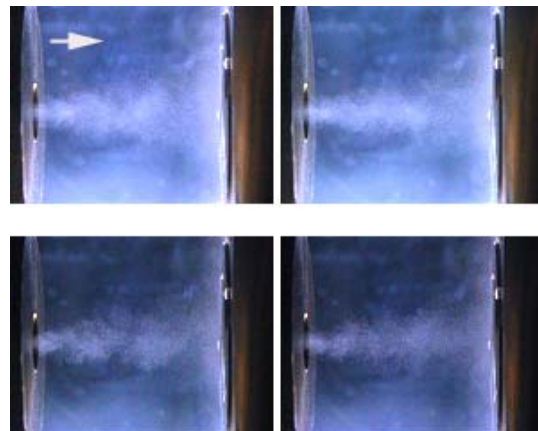


Figure 3. Cavitating jet started inside the nozzle and appears as jet comprised only of very tiny individual bubbles and with a big spreading angle, $p_1 = 8 \text{ bar}$, $p_2 = 2.05 \text{ bar}$, $\sigma = 17.85$, $v_j = 4.9 \text{ m/s}$, $T = 16^\circ\text{C}$, Divergent Nozzle ($d_{in} = 45\text{mm}$, $d_{out} = 1\text{mm}$).

Some differences between the two cases (divergent and convergent) can be noted. The jet penetration in the convergent conical nozzle is more intensive than that in the divergent case, for all the upstream pressures ($p_1 = 45, 95, 145$ and 195 bar). This is attributed to the big differences in the velocities for the two nozzle directions (divergent and convergent), so this also represents the velocity effect. For convergent nozzle the

jet breaking-off usually started at a distance greater than 35% of the distance between the nozzle lip and the target surface and at higher upstream pressures ($p_1 \geq 100$ bar).

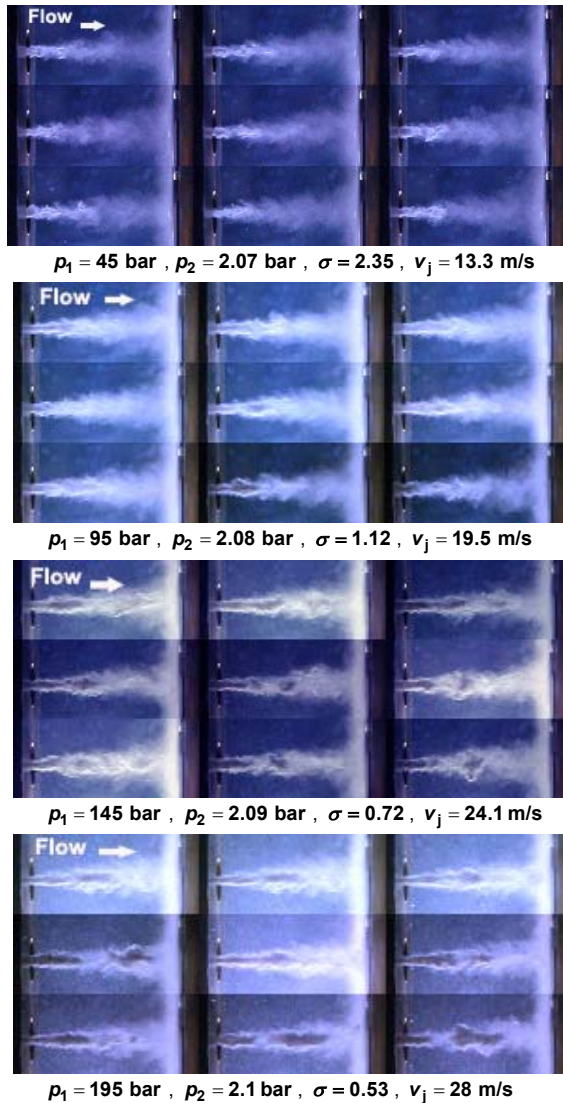


Figure 4. Cavitating jet started outside at the nozzle lip and appears as jet comprised of very tiny individual bubbles and cavitation clouds. $T = 16^\circ\text{C}$. Divergent nozzle ($d_{in}=45$ mm , $d_{out}=1$ mm).

At the same upstream pressure $p_1 = 8$ bar , divergent nozzle produces a jet that contains tiny distributed bubbles and has the shape of a funnel (Fig.3), while for the convergent nozzle at the same upstream pressure no jets or cavities could be observed. However, for convergent nozzle, with upstream pressure increased ($p_1 \geq 20$ bar) and downstream pressure fixed at $p_2 = 1$ bar , the cloud cavitation appeared at the nozzle lip. This cavitation was unstable and appeared with irregular and very rare frequency. The images for convergent conical nozzle at $p_1 = 8$ bar and $p_1 = 20$ bar are not shown in the paper since no regular phenomenon (cavitation) appeared at these conditions, so they may represent only the inception of cavitation.

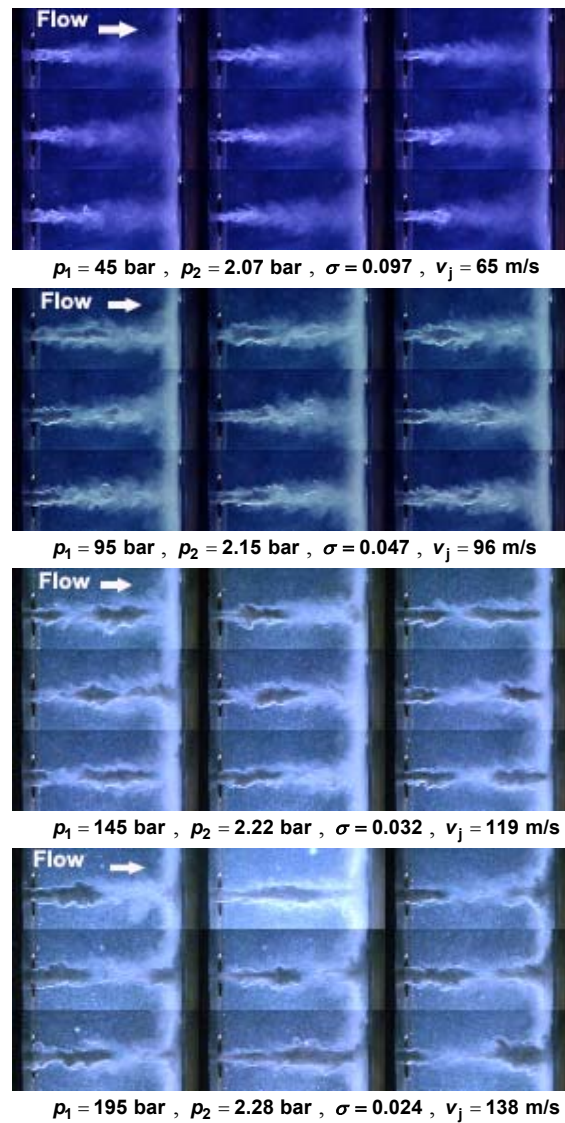


Figure 5. Cavitating jet started outside at the nozzle lip and appears as jet comprised of very tiny individual bubbles and cavitation clouds. $T = 16^\circ\text{C}$. Convergent nozzle ($d_{in}=1$ mm , $d_{out}=0.45$ mm)

For the cases of convergent nozzle at $p_1 = 145$ and 195 bar, many bubbles are distributed throughout the whole area. This feature is related to the intensive vortices action in the jet, which leads to liberation of bubble growth, spreading and floating in the chamber. Finally, these bubbles collapse when they meet the point of sufficient pressure in their path. However, these gas bubbles have longer lifetime as compared to cavity bubbles and they do not contribute to the cavitation erosion.[14]

The nozzle direction (convergent or divergent) has a significant influence on the jet width and jet spreading angle. Comparison of the images for the two cases shows that the jet width and its spreading angle are bigger for the case of divergent nozzle, supporting the presumption that the cavitating jet is a combination of big cavities (clouds) and the bubbles, which are surrounding the cavity clouds.

3.2 Influence of Nozzle Dimensions on Cavitating Jet Behavior

As the influence of nozzle geometry is very significant for the jet behaviour, it is to be understood that this geometry is not only reflecting itself in a way of sudden expansion or sudden convergence, but also in a way of different diameters, length, etc. of a certain nozzle. As an example, in this section only, the analysis will be shown for a divergent nozzle only (fixed as shape - sudden divergence), but with different inlet and outlet diameters (exact data given as captions of Figs. 6 and 7). Upstream pressure was kept constant, as well as temperature and standoff distance, while jet velocity and downstream pressure changed with the nozzle geometry (thus the cavitation number also changed).

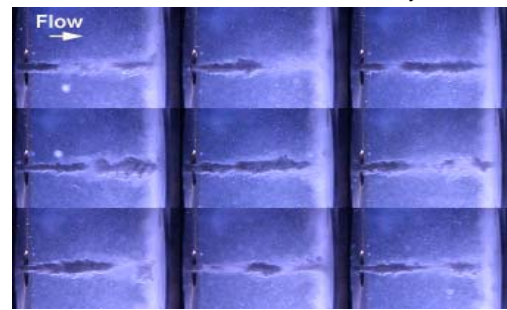
The comparison between the images in Fig.6 and Fig.7 reveals that the cavitating jet characteristics are strongly dependent on geometry (diameters of the nozzle) - jet penetration, jet width, jet spreading angle and cavitation cloud density are the cavitating jet features that change significantly. Change in the nozzle geometry leads to the change of the most important parameters for cavitation such as downstream pressure, jet velocity and pressure distribution in the test chamber. In addition, the jet width, jet spreading angle and cavitation cloud density are decreased as the inlet nozzle diameter is decreased. The cavitation number σ used in the paper is calculated by the definition $\sigma = [(p_2 - p_v) / (0.5 \cdot \rho \cdot v_j^2)]$. Values found in that way are different for Figs. 4 and 5, where the group of photos in Fig.4 were taken for such a σ which is greater than the ones for the group of photos in Fig.5. If the definition of σ proposed by ASTM ($\sigma = p_2 / p_1$) would be applied, the result for σ will be the opposite. This also proves that geometry is a very important influencing factor since in the first definition it influences through the value of velocity, while in the second it is hidden somewhere or is not considered at all.

Visualization of the cavitation in Figs. 6 and 7 allows for comparison of the images. Images in Fig. 7 show more intensive cavitation than those in Fig. 6 although σ numbers are higher for images in Fig. 7 than in Fig. 6, if the ASTM definition ($\sigma = p_2 / p_1$) is used. So, the differences between images in Figs. 6 and 7 represent influence of nozzle dimensions. In addition, definition, it is evident that the ASTM definition is not a proper one and it is better to use the normal definition for describing the phenomenon.

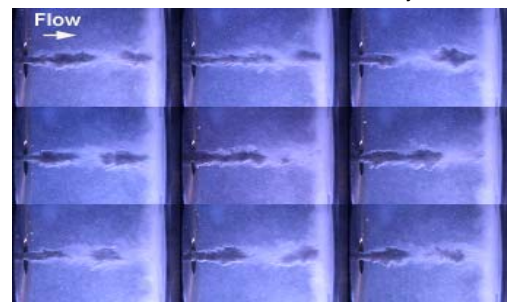
The existence of two types of cavitation (gaseous and vapour) at high upstream pressures may be noticed in the group images at $p_1 = 145$ and 195 bar in Figs. 4 and 5. The gaseous type seems to be formed in the entire jet with bubbles of nearly spherical shape which did not form clusters. This type of cavitation is mainly dependent on upstream pressure p_1 . The vaporous type of cavities strongly depends on cavitation number and relatively large coalescing vaporous cavities may form away from, nearby or possibly inside the nozzle itself.



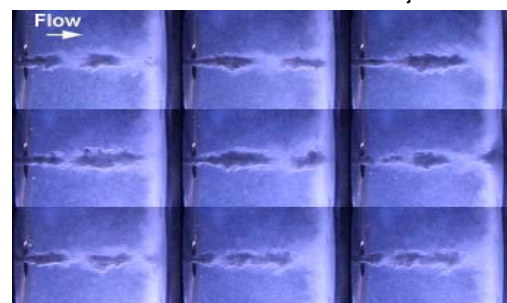
$p_1 = 45 \text{ bar}$, $p_2 = 1.92 \text{ bar}$, $\sigma = 1.93$, $v_j = 14 \text{ m/s}$



$p_1 = 95 \text{ bar}$, $p_2 = 1.99 \text{ bar}$, $\sigma = 0.95$, $v_j = 21 \text{ m/s}$



$p_1 = 145 \text{ bar}$, $p_2 = 2,1 \text{ bar}$, $\sigma = 0,64$, $v_j = 25 \text{ m/s}$



$p_1 = 195 \text{ bar}$, $p_2 = 2.2 \text{ bar}$, $\sigma = 0.5$, $v_j = 29 \text{ m/s}$

Figure 6. Cavitating jet started outside at the nozzle lip and appears as jet comprised of very tiny individual bubbles and cavitation clouds. $T = 16^\circ\text{C}$. Divergent nozzle ($d_{in} = 0.55 \text{ mm}$, $d_{out} = 1 \text{ mm}$)

Another interesting difference between the two types of cavitation is that the vaporous cavities disappear after a certain distance from the nozzle lip, while the gaseous bubbles tend to persist indefinitely (only an increase of p_2 destroys them). As in Knapp R.T. et al. (1970) and Vijay M. et al. (1991), it was found that gaseous cavities do not contribute to the erosion of material.

Again, comparison between the images in Figs. 6 and 7 also explains the influence of nozzle geometry on cavitation behaviour since for these cases the outlet diameters d_{out} are equal, but inlet diameters d_{in} are different.

3.3 Influence of Cavitation Number (σ) (Exit Jet Velocity) on Characteristics of Cavitating Jets

In order to get better distribution of light, the flash light and the camera eye were installed on the same side (same window).

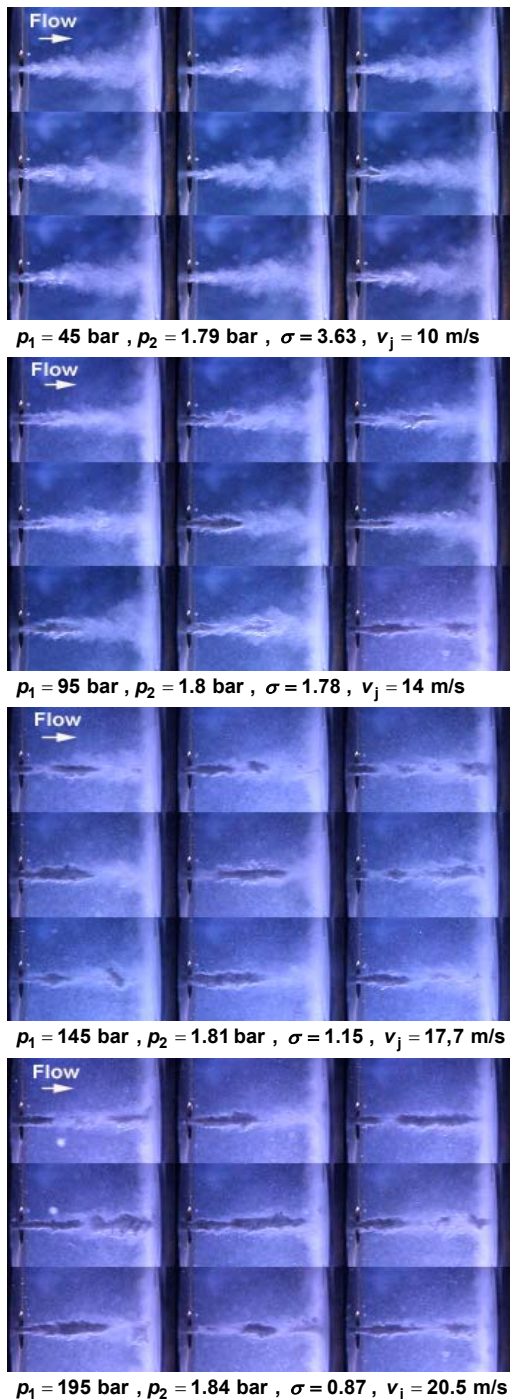


Figure 7. Cavitating jet started outside at the nozzle lip and appears as jet comprised of very tiny individual bubbles and cavitation clouds. $T = 16^{\circ}\text{C}$. Divergent nozzle ($d_{in} = 0.4 \text{ mm}$, $d_{out} = 1 \text{ mm}$)

Since the window area was not enough to accept the camera and the flash together in parallel, in order to improve the quality of images, the flash had to be

inclined to the camera direction with in-between angles (θ) of 30° and 30° .

The experimental installation is shown on the side of Fig.2 (right). Visualizations were done with convergent conical nozzle and for different cavitation numbers σ , which was achieved by changing the downstream pressure.

Figs. 8 and 9 show the cavitating jet at different cavitation numbers σ at constant velocity and with velocity not constant respectively. The visual analysis reveals that the jet appears as a complete solid unit in white colour – it looks like a peice of white granite.

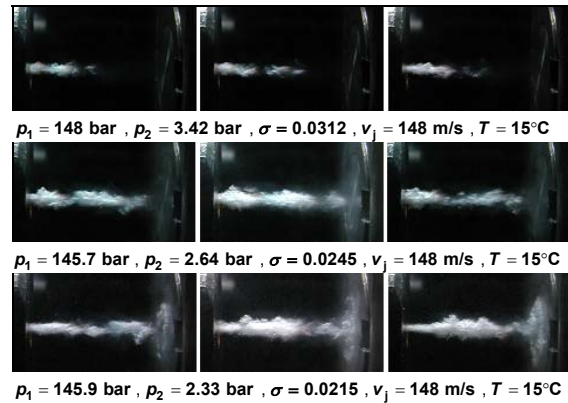


Figure 8. Influence of cavitation number on the jet appearance.

The jet penetration is increased as σ or P_2 is decreased and when jet strikes the target it starts spreading over the target surface and formation of rings appears. In the first row in Fig.8 the jet did not arrive to the target wall – it disappeared in the region of the second third of the full distance between the nozzle lip and the target wall ($2/3$ of x). The breaking-off point is shifted to downstream and jet width increases as σ or p_2 is decreased. This result is in good agreement with Soyama's results. In the second and third row of images in Fig. 8 and the third, fourth and fifth row of images in Fig. 9, the gaseous bubbles appear as fog distributed in the chamber.

3.4 Influence of Visualization System Position on the Information Content in Cavitating Jet Images

The visualization process used in the paper was a tool to get as much as possible information on the cavitating jet phenomenon. In order to improve the understanding of phenomenon, the influence of the position of visualization system on the information of the cavitating jet was analysed.

In the first case the visualization was made with a sheet of white paper in-between the flash and the window. The reason for this was to reduce the amount of light that illuminates the jet when passing to the camera eye. In addition, the paper enhances the distribution of the light in the test chamber (Fig.10 (down) shows the setup). In the second case the visualization was made by mounting the flash in such a way to be in parallel with the jet direction (in the direction same with the flow). The light was from the

other side of the test chamber with the angle $\varphi = 90^\circ$ to the camera eye without any paper put in-between and the flash was cross-axial with the camera, as shown in Fig.10 (upper).

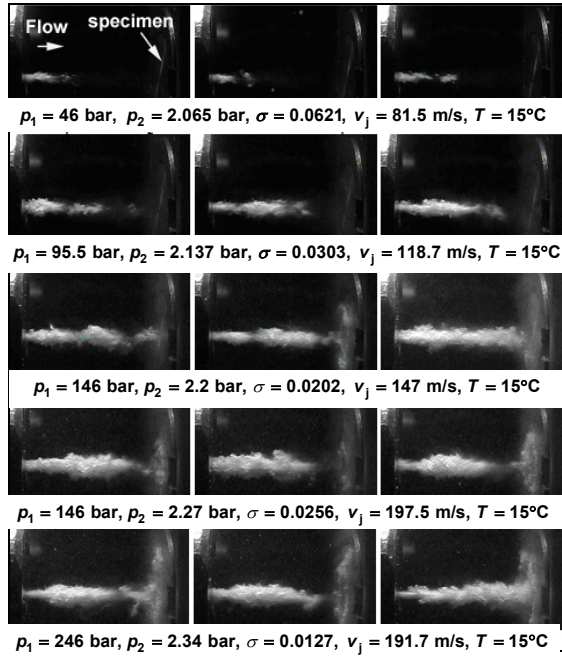


Figure 9. Influence of exit jet velocity (v_j) on the jet appearance.

The investigation was done at three upstream pressure values $p_1=100, 152$ and 203 bar for both cases of visualization system positions. The convergent conical nozzle was used and the images are presented in Figs.11, 12 and 13. Photos in the second column in each figure were gained by the first way of installation, while photos in the first column in each figure were gained by the second way of installation.

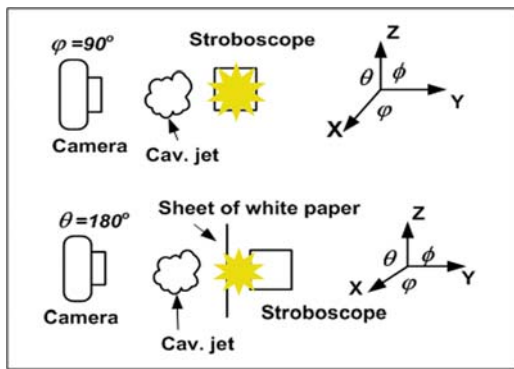


Figure 10. Visualization system arrangement.

The comparison between the two cases reveals that the position of light and its distribution is a very important factor in the information established by visualization process for the cavitating jets.

In the first case the cavitating jet appears as a dark grey shadow. It seems less dense and punched in some locations. The difference in the jet aspects compared with the second case may be attributed to the pass of

some light through the jet, so the jet as a complete solid unit cannot be seen in this case. Also, there exists a reflection process of light by the spherical bubbles in or around the jet. However, this reflection is not in the direction of camera eye, so the camera does not sense the reflected light. All of these reasons, including the limitation of camera resolution, contribute to the fact that bubbles will not appear in the images and the jet appears as a dark grey shadow.

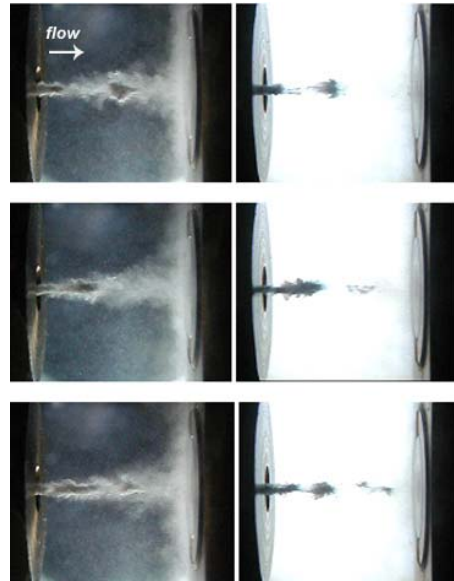


Figure 11. Influence of apparatus arrangement on the jet characteristic information, $p_1=95 \text{ bar}, p_2=2.08 \text{ bar}, \sigma = 1.12, v_j = 19.5 \text{ m/s}, T = 16^\circ\text{C}$ (Divergent nozzle)

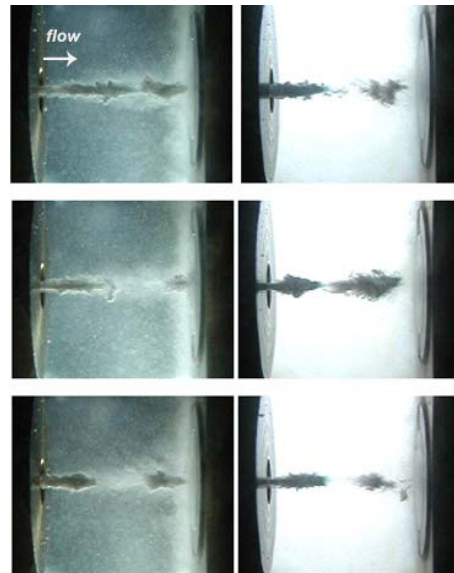


Figure 12. Influence of apparatus arrangement on the jet characteristic information, $p_1=145\text{bar}, p_2=2.09 \text{ bar}, \sigma = 0.72, v_j = 24.1 \text{ m/s}, T = 16^\circ\text{C}$ (Divergent nozzle)

In the second case, when flash was mounted in a way to be perpendicular to the camera eye and at the same time to be perpendicular to the jet flow direction (i.e. the angles were $\theta = 90^\circ$ and $\phi = 90^\circ$, respectively, as in Fig.2 (right)), the light was reflected by the

spherical bubbles, and thus the distances between the cavitation clouds (or clusters of bubbles), produced during the break off, were allowed to be seen. The rest of the jet appears as a rear white distance and it contains a lot of tiny bubbles that may reflect some light to the direction of the camera eye. At $p_1 = 152$ bar, the gas bubbles appear in the images obtained with the flash parallel to the jet flow direction. They do not appear in the group of images obtained in the first case. At $p_2 = 203$ bar, the gas bubbles appear in both cases, which may be explained by the appearance of a greater number of bubbles at pressure $p_2 = 203$ bar than at $p_1 = 152$ bar. But the bubble density (number of bubbles) which appears in the images obtained in the first case is much less than that which appears in the images obtained by the second case.

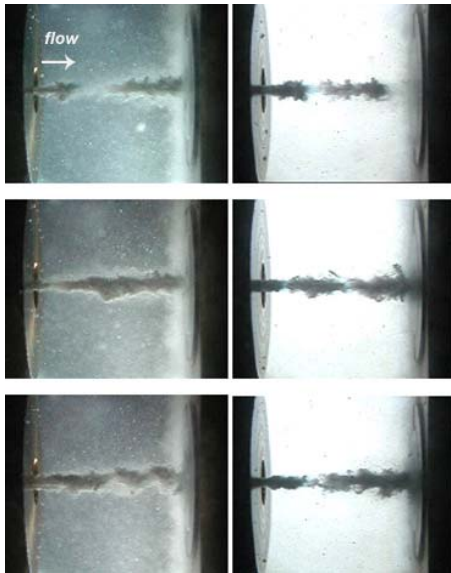


Figure 13. Influence of apparatus arrangement on the jet characteristic information, $p_1=195$ bar, $p_2=2.1$ bar, $\sigma=0.53$, $v_1=28$ m/s, $T=16^\circ\text{C}$ (divergent nozzle)

4. CONCLUSION

The jet behavior and its features depend on nozzle mounting (convergent or divergent way). The hydrodynamic conditions for cavitation inception and its position depend on the nozzle geometry. The hydrodynamic condition has a big influence on the jet behavior and its features. Both gaseous and vaporous types of cavitation appear at high upstream pressures. The life of gaseous cavitation is longer than of vapor cavitation. Vaporous types of cavitation depend on cavitation number or on downstream pressure P_2 , while gaseous cavitation depends mainly on upstream pressure P_1 . Both of them depend on the nozzle geometry. The position of the visualization system and its quality has great influence on the quality of jet images and information. The difficulties of catching the collapsing moment of the bubbles are related to two reasons: the first is inadequate temporal resolution of illuminating and recording system, and the second is the huge number of the bubbles in the cavity.

REFERENCES

- [1] Conn, A.F., Johnson, V.E., William, Jr., Lindenmuth, T., Fredrick, G.S.: Some Industrial Applications of Cavitating Fluid Jets Flow, Proceedings of the First U.S. Water Jet Conference Golden, Colorado, pp. 238-253, 1981.
- [2] Ganippa, L.C, Bark, G., Andersson, S., Chomiak, J.: Comparison of Cavitation Phenomena in Transparent Scaled-Up Single-Hole Diesel Nozzles. CAV2001, California, USA, Session A9.005, June, 2001
(<http://cav.2001.library.caltech.edu/>)
- [3] Kato, H., Yamaguchi, H., Maeda, M., Kawanami, Y., Nakasumi, S.: Laser Holographic Observation of Cavitation Cloud on a Foil Section. Journal of Visualization, Vol.2, No.1, July, 37-50, 1999.
- [4] Keiichi, S., Yasuhiro, S.: Unstable Cavitation Behaviour in a Circular-Cylindrical Orifice Flow. Trans JSME, International Journal, Ser. B, Vol. 45, No. 3, pp.638-645, 2002.
- [5] Knapp, R.T., Daily, J.W., Hammitt, F.G.: *Cavitation*, McGraw-Hill, New York, 1970.
- [6] Ran, B., Katz, J.: Pressure Fluctuation and Their Effect on Cavitation Inception within Water Jets. ASME, FED-Vol 177, pp. 31-42, 1993.
- [7] Soyama H. High-Speed Observation of a Cavitating Jet in Air. Trans ASME, Journal of Fluids Engineering, Vol. 127, pp 1095-1101, November 2005.
- [8] Soyama, H., Adachi, Y., Yamauchi, Y., Oba, R.: Cavitation-Noise-Characteristics Around High Speed Submerged-Water-Jets, Trans. JSME (B), Vol. 60, pp. 730-735, 1994.
- [9] Soyama H, Ikohagi T, Oba R. Observation of the Cavitating Jet in a Narrow Watercourse. Cavitation and Multiphase Flow. ASME, FED-Vol.194, 79-82, 1994.
- [10] Soyama, H., Lichtarowicz, A., Lampard D. Useful Correlations for Cavitating Jets. 3rd International Symposium on Cavitation, Grenoble, France, pp. 17-24, 1998.
- [11] Soyama, H., Yamauchi, Y., Adachi, Y., Adachi, Y., Oba, R.. High-Speed Cavitation-Cloud Observations Around High-Speed Submerged Water Jets, The second international Symposium on Cavitation, Tokyo-Japan, pp. 225-230, 1994.
- [12] Soyama, H., Yamauchi, Y., Adachi, Y., Adachi, Y., Oba, R.: High-Speed Cavitation-Cloud Observations Around High-Speed Submerged Water Jets, Trans JSME, International Journal, Ser.B, Vol.38, No.2, pp.245-251, 1995.
- [13] Toyoda, K., Muramatsu, Y., Hiramoto, R.: Visualization of the Vortical Structure of a Circular Jet Excited by Axial and Azimuthal Perturbation, Journal of Visualization, Vol.2, No.1, July, pp. 17-24, 1999.

- [14] Vijay, M.M., Zou, C., Tavoularis, S.: A Study of the Characteristics of Cavitating Water Jets by Photography and Erosion. Jet Cutting Technology, Proceedings of the Tenth International Conference, pp. 37-67, Elsevier, 1991.
- [15] Yamaguchi, A., Shimizu, S.: Erosion Due To Impingement of Cavitating Jet. Trans ASME, Journal of Fluids Engineering, Vol.109, pp. 442-447, 1987.

NOMENCLATURE

σ	cavitation number, $\sigma = \frac{p_{\text{ref}} - p_v}{0.5 \cdot \rho \cdot u_{\text{ref}}^2}$
p_{ref}	reference (downstream) pressure [bar]
$p_v(T)$	saturation (vapour) pressure [bar],
$\rho_L(T)$	density of the liquid [kg/m ³],
T	fluid temperature [°C]
u_{ref}	reference velocity - exit jet velocity [m/s] $u_{\text{ref}} = Q / A = v_j$
q_V	flow rate (m ³ /s) $q_V = K \cdot \sqrt{(p_1 - p_2)}$
A	nozzle outlet cross-section area [m ²]
p_1	upstream pressure [bar], (absolute)

p_2	downstream pressure [bar], (absolute)
X	stand-off distance [mm]
L	nozzle length
$d_{\text{in}}, d_{\text{out}}$	inlet and outlet nozzle diameter [mm]
K	= 4.78E-09 for divergent ; = 6.17E-09 for convergent nozzle [m ³ /s/Pa ^{1/2}]

ИСТРАЖИВАЊЕ ПОНАШАЊА ПОТОПЉЕНОГ КАВИТАЦИОНОГ МЛАЗА: ДРУГИ ДЕО – УТИЦАЈИ РАДНИХ УСЛОВА, ГЕОМЕТРИЈСКИХ ПАРАМЕТАРА И НАЧИНА ПОСТАВЉАЊА СИСТЕМА ДЕТЕКЦИЈЕ

Ezddin Ali Farag Hutli, Милош Недељковић

На основу резултата визуелизације кавитационог воденог млаза добијених дигиталном камером, истраживани су утицаји параметара као што су: притисак убризгавања, пречник и геометрија млазнице, начин постављања млазнице (конвергентан или дивергентан), кавитацијског броја и излазне брзине млаза. Додатно је проучаван ефекат постављања система за визуелизацију. Показан је јак утицај свих параметара на изглед млаза и његове карактеристике.